Thermogenetics for cardiac pacing

Alexander V. Balatskiy, Alexey M. Nesterenko, Aleksandr A. Lanin, Vera S. Ovechkina, Semyon S. Sabinin, Elena S. Fetisova, Alexander A. Moshchenko, David Jappy, Rostislav A. Sokolov, Diana Z. Biglova, Georgy M. Solius, Ekaterina M. Solyus, Sergei V. Korolev, Oleg V. Podgorny, Ilya V. Kelmanson, Andrei V. Rozov, Andrei B. Fedotov, Tobias Bruegmann, Alexei M. Zheltikov, Andrey A. Mozhaev, Vsevolod V. Belousov

Abstract

Cardiac arrhythmias are common disorders that can be fatal. Modern methods of treating bradyarrhythmias include the implantation of pacemakers and cardioverters – defibrillators. However, the implantable devices can cause various complications including infectious ones, related to the electrodes installed inside the heart. Less invasive heart rhythm modulation could be beneficial for some cohorts of patients. We present an alternative approach to heart pacing based on thermogenetics. We used adeno-associated viruses to deliver genetic human transient receptor potential subfamily V member 1 (TRPV1), a heat-sensitive cation channel, into isolated cardiomyocytes and the mouse heart. This allowed us to induce action potentials and control contractility using short heat pulses delivered by infrared laser illumination. Using this approach, we demonstrated the thermogenetic pacing of isolated cardiomyocytes *in vitro* and in the mouse heart *in vivo*. Our results demonstrate the unique potential of thermogenetics for developing novel therapeutic strategies for heart rhythm modulation.

Introduction

Electrical stimulation of cardiomyocytes and cardiac tissue is the gold standard for laboratory studies and clinical applications. In patients, implantation of electrical devices, such as pacemakers or cardioverter-defibrillators, is very common, in some countries the implantation rate is >1000 cases per million people[1]. According to some estimates, more than 1 million devices are implanted worldwide annually[2].

Nevertheless, electronic pacemakers have significant limitations, such as the need for an invasive surgical procedure, the risk of infections, device failure, regular battery replacement, and electrochemical reactions at the electrode contact sites. In addition, there is the possibility of endocarditis, thrombosis, electrode dislocation, and other complications both in the early postoperative and long-term periods. Automatic cardioverter-defibrillators, when triggered, generate extremely painful discharges for the patient, leading to significantly decreased quality of life. In a recent study, major complications occurred in 8.2% of patients after the implantation of pacemaker or defibrillator within 90 days of hospital discharge[3].

Thus, there is a need for alternative approaches to reduce complications associated with device implantation. As alternative solutions for the correction of cardiac arrhythmias, there are approaches using gene and cell therapy[4–6]. Nowadays the emergence of a variety of genetically encoded tools has opened the possibility of studying and controlling the activity of nerve, muscle, and secretory cells by exposing ectopically expressed molecular targets to chemical ligands, light, or temperature fluctuations. Technologies using such principles of action are known as chemogenetics, optogenetics, and thermogenetics. The advantage of these technologies is the possibility of targeting certain groups of cells with high spatial resolution using tissue-specific promoters.

Optogenetic methods using photosensitive proteins to control cardiomyocyte contractions have been applied to isolated cardiomyocytes[7,8], zebrafish hearts[9], transgenic mouse hearts[10], and *ex vivo* mouse hearts with intramyocardial transgene delivery by AAV[11,12]. Despite the existing options for the use of optogenetics on cardiomyocytes, this technology has significant limitations and disadvantages. First, optogenetics uses rhodopsin ion channels that need to be activated by visible light. Research aimed at developing redshifted channelrhodopsins is far from identifying effective deep-penetrating activation radiation since most studies still use visible light to activate the widely used channelrhodopsin 2 (ChR2)[13–15]. This leads to the fact that the stimulation of cells in optically opaque animals in the vast majority of cases is invasive, using implantable devices such as optical fibers. Despite approaches to the creation of rhodopsins with high conductivity[16], most have low conductivity[17] and

require a high level of channel expression and a high intensity of activating light, which can lead to phototoxic effects. Second, a no less significant disadvantage that limits the use of the *in vivo* optogenetic approach is the use of channelrhodopsins which are not found in mammalian organisms and can cause an immune response and, as a result, rapid death of the cells expressing them[18,19].

Thermogenetics is a promising alternative approach based on the use of non-selective cation channels, which can be opened by temperature change[20]. The advantage of using these channels is that they are present in mammals, which makes an immune response much less likely. These channels are found in many tissues and cells, some are present on the membranes of sensory neurons, acting as thermal sensors, and in some cases, pain receptors, in various groups of animals. These channels also have a significantly higher conductance compared to ChR[21]. The high conductivity and ability of some to respond to small temperature shifts of 1–2°C have contributed to the use of these channels as thermogenetic activators of various cells. The advantages of thermogenetics also include the wide range of ways to activate thermosensitive channels: infrared (IR) radiation[22–24], microwaves[25], focused ultrasound[26] or magnetic nanoparticles in an alternating magnetic field[27]. Previously, the possibility of IR laser stimulation of single cells with the possibility of generating successive action potentials on a millisecond scale, commensurate with the response time of light-sensitive channels of optogenetics, was demonstrated[24].

In the present study, we applied a thermogenetic approach to control the rhythm of isolated cardiomyocytes *in vitro*, and the mouse heart *in vivo* using pulsed IR laser heating, based on the use of human transient receptor potential subfamily V member 1 (TRPV1). Our study demonstrates that TRPV1 is an excellent tool for thermogenetics and has the potential for a wide range of future applications from research to therapeutic interventions.

Results

Thermogenetic pacing of cardiomyocytes in vitro

We chose the human transient receptor potential cation channel subfamily V member 1 (hTRPV1) channel as a thermogenetic instrument. When heated to 41–43°C, it opens and passes Na^+ and Ca^{2+} through the plasma membrane into the cell, which leads to depolarization. We hypothesized that this depolarization can trigger action potentials in cardiomyocytes. To demonstrate thermogenetic activation *in vitro*, we expressed the truncated version of hTRPV1 in neonatal murine cardiomyocytes. We transduced cells with AAV-PHP.S containing cTnT_hTRPV1(–109aa)_P2A_mRuby. This truncated channel demonstrated the same activity as the full-length hTRPV1. The activation of hTRPV1(−109aa) in HEK293 cells heated by a nichrome wire loop is shown in Fig. S1. The activation of cells expressing the full-length hTRPV1 using the same method was earlier demonstrated by our team (under review, the preprint is available upon request).

To heat cardiomyocytes, we used an IR laser connected to an optical fiber fixed on a micromanipulator. We gradually increased the pulse duration and power until the pacing was achieved. The average pulse characteristics used for successful pacing are given in Table S1 and are shown in detail in Fig. S2. The entire dataset is deposited[28]. Electrophysiological measurements demonstrated action potentials induced by laser-induced heat pulses at frequencies up to 7 Hz (Fig 1A, B). This coupling was absent in control cells (non-transduced or transduced with cTnT_GCaMP6s, Fig 1C). Application of 100 μM capsaicin through a pipette within about 20 μm of the recorded cell led to rapid and long-lasting depolarization in cells transduced with cTnT_hTRPV1(−109aa)_P2A_mRuby but not in the control cells (Fig. 1D). All inward currents were completely abolished by the selective TRPV1 inhibitor AMG517 (1 μM solution applied through a pipette near the cell), (data not shown). The statistical analysis did not reveal any correlation between pulse characteristics and successful pacing, probably due to the heterogeneity of the primary culture

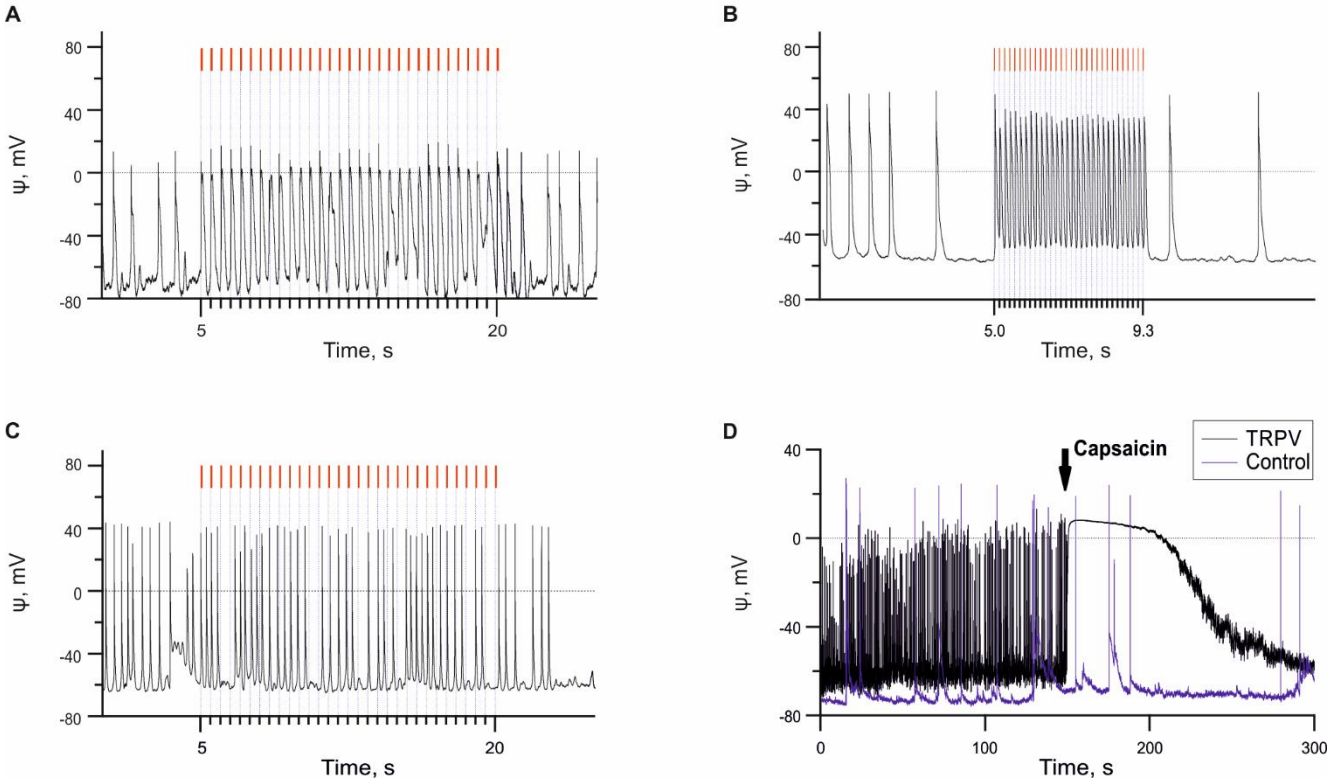

Figure 1. Thermogenetic pacing of isolated neonatal murine cardiomyocytes using IR laser (the amplitudes of the laser pulses (red) are arbitrary). **A.** Depolarization of cardiomyocytes transduced with hTRPV1(−109aa) induced heat pulses with a repetition rate of 2 Hz . **B.** Depolarization of cardiomyocytes expressing hTRPV1 induced by 7 Hz heat pulses. **C.** Heating of control cells transduced with GCaMP6s. **D.** Addition of capsaicin to cells transduced with hTRPV1, and to control cells transduced with GCaMP6s.

Thermogenetic heart pacing in vivo

All experiments were performed four weeks after injection of AAVs carrying cTnT_hTRPV1-FLAG. Mice did not demonstrate signs of pathology up to 3 months after the injection. Open hearts of anesthetized and ventilated mice were heated with laser pulses. In animals transduced with cTnT_hTRPV1-FLAG, the shape of ventricular complexes changed and heartbeats were synchronized with heat pulses at frequencies up to 6 Hz (Figs. 2a, 2b). In control mice, complex shapes were also slightly affected but the heart rate was not modified during IR laser treatment (Figs. 2c, 2d). Note, synchronization (phase locking, “L” in Figs. 2a, 2b) occurred 10–20 sec after the beginning of pacing. In contrast to cell culture in a Petri dish, the heart is an object with a large thermal capacity, leading to a baseline temperature increase up to 40°C at about 12 sec after the beginning of the laser pulse train irradiation. Above this drift there are sharp temperature spikes with a magnitude of 3°C and a duration of 50 ms, the same as the laser pulse width. These small pulses allow hTRPV1 activation temperature threshold to be reached (Fig. 2C–D). We used the same IR laser setup for experimental animals. With our setup, we had to use the maximum possible laser power to reach the target temperature in a short time, so we didn’t have much flexibility in choosing the heating parameters. The statistical analysis did not reveal any correlation between pulse characteristics or the initial frequency and successful pacing (Table S2).

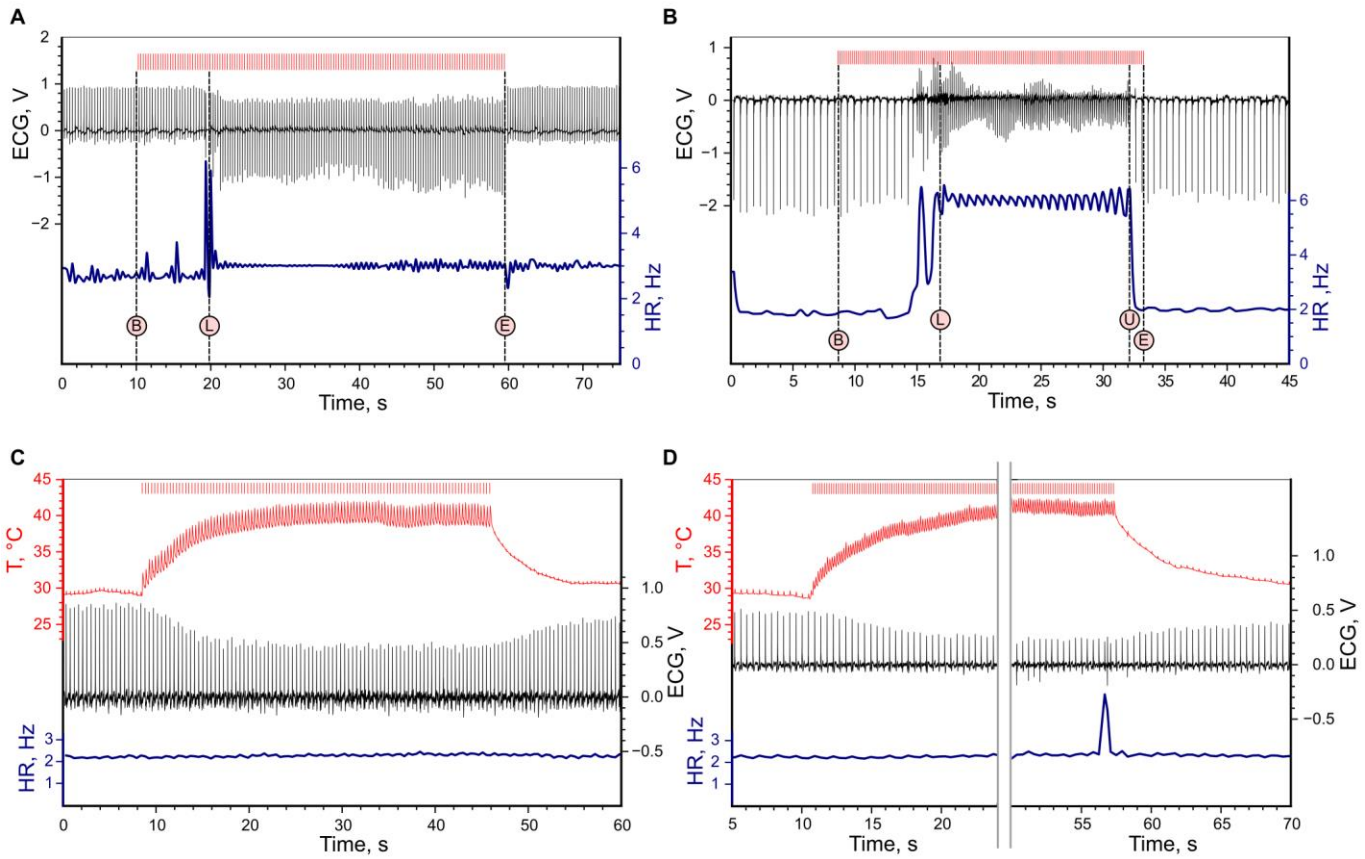

Figure 2. Thermogenetic heart pacing *in vivo* using apex heating by IR laser pulses. Denoised ECG (black lines) and heart rate (HR, blue lines) are depicted for experimental animals with hTRPV1 expression (**A**,**B**) and control animals (**C**,**D**). IR 3 Hz (**A**,**C**) and 6 Hz (**B**,**D**) laser pulses were applied (top red dashes). Temperature was measured only in control animals (red curve). Events are labeled with circles: 'B'/'E' — beginning and ending of pulse sequence, 'L'/'U' — phase locking/unlocking.

During pacing of the atrium the imposed frequency was held very precisely and the phase locking was set very quickly (Fig. 3). Firstly the pulse was located at the very end of the R-R interval so that the atrium contracted in the middle of trigger pulse duration (Fig. 3C). The further the pacing progressed, the more the pulse moved backward from the consequent R-peak. Finally the pulse reached the position when its end corresponded approximately to the position of the P-peak (Fig. 3D). The described behavior is general and not unique to this sample, we provide different data samples deposited[29] (see also Table S2). Initial phase locking probably occurred when the cells in the atrium reached a target temperature and a critical amount of cells depolarized. In this case, the P-peak was located approximately 40 ms after the laser pulse. After the action potential has already developed and the atrium has already contracted, prolonged heating can only cause a calcium overload. The heart probably may adapt its behavior to develop action potentials only when the heating is already finished.

In contrast to pulsed IR illumination, constant heating of the atrium by the IR laser induced a very unstable beat with a high variability of complex shape (Fig. S4C–C'). In addition, increased heart rate was also observed in control hearts as well. The reaction of control hearts during pacing with typical parameters is shown on Fig. S3. Heart rate was considerably increased (Fig. S3B), however no synchronization of laser peaks with heart beating was detected (Fig. S3A). Heating of ventricular tissues in control hearts did not affect the rhythm in both pulsed and continuous modes (Fig. 2C,D and Fig. S7), but affected the amplitude of the R-peak (Fig. 2C,D).

In control recordings we were able to observe typical heating of cardiac tissues measured with a probe. In the case of atrium pacing, the phase locking in experimental animals was achieved in a much shorter time (in 1–2 seconds) than it took for the atrium to reach the threshold temperature (~10 sec) (Fig. S2B). Cells at the surface of the atrium were probably heated quicker than the entire atrium, providing initial depolarization sufficient for pacing.

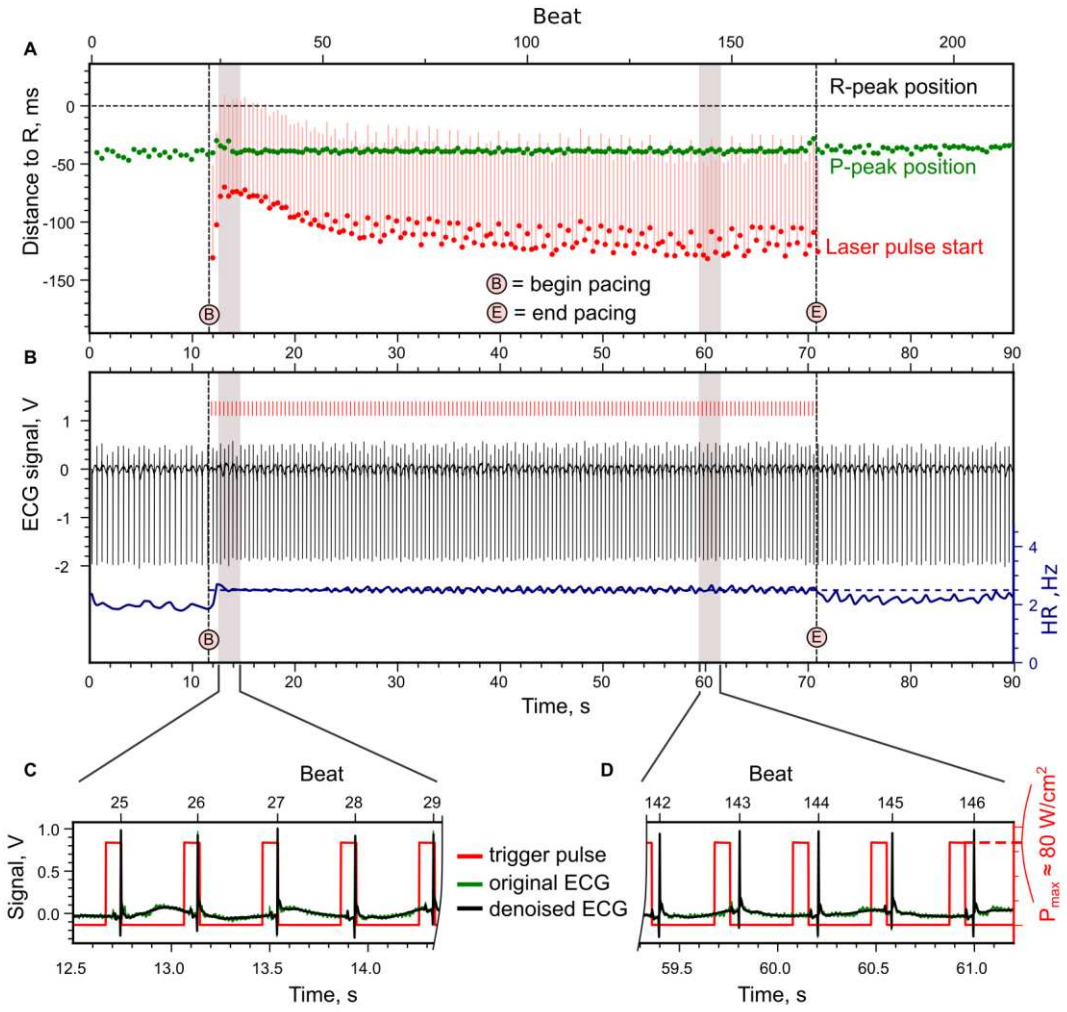

Figure 3. Typical example of atrium pacing with a frequency slightly higher than the intrinsic one. Pacing was at 2.5 Hz with 80 ms pulses, initial HR was ~2 Hz. **A.** Position of the P-peak and laser pulse in relation to the R-peak in ms. Negative values mean that events occur *before* the reference peak. **B.** Change of complex shape (black curve) and heart rate (blue curve) during the experiment. Vertical red lines demonstrate the pulse widths of the trigger pulses. **C.** ECG signal and trigger pulses in short intervals corresponding to the beginning and ending parts of the pacing. The positions of the intervals are indicated with gray bars in panes **A** and **B**.

Rhythm imposing peculiarities and calcium dynamics in cardiomyocytes

For most patients, heart pacing therapy is required chronically. Therefore, it is important to evaluate potential problems of a new technology that should be addressed before it is transferred to a clinic. For thermogenetic heart pacing we report two major problems observed so far: incomplete phase locking and loss of phase locking during long-time pacing.

We recorded a lot of samples with accurate heart pacing (Table S2) with S:R = 1:1 phase locking (S : R means Stimulus : Response). However, in many cases phase locking was incomplete, some laser pulses initiated a heart beat and others were skipped. In atrium pacing experiments, there were events of incomplete phase locking with S:R being 4:3 or 3:2. In Fig. 4 we show an example of 1:1 phase locking turning into 4:4 (which means that each laser pulse corresponds to P and R peaks, but the times between pulses and peaks are different) and then to 4:3 phase locking. First, we observe that every fourth beat occurs slightly earlier than the other three beats (Fig. 4A, 10 – 15 sec). Since every pulse in this case occurs inside a distinct RR interval, we consider this locking as 4:4. The difference between fourth intervals and others smoothly grows and then phase locking changes (event "R") to 4:3. In this mode, two laser pulses induce two responses and then the next two laser pulses lay within the next R-R interval (Fig. 4C). Interestingly, the first two pulses end with P-peaks, i.e. they induce atrium contraction,

whereas the last two pulses of the cycle lay within 3rd large R-R interval and the second one ends with R-peak, i.e. these peaks cumulatively induce ventricular contraction synchronously with the atrium. In this way, 4 laser pulses are coupled with 3 contractions. Moreover, the first R-R interval in this 3-point cycle corresponds to the stimulation frequency whereas the last one (containing two laser pulses inside) corresponds to the intrinsic frequency. In other words, the heart tries to support both the intrinsic and imposed rhythms at the same time if the stimulation is not intense enough to strictly impose the faster rhythm.

During the pacing series longer than 40 s, especially when the ventricle was paced, we observed spontaneous loss of synchronization. In some cases, pacing was spontaneously restored (Fig. S5). This phenomenon was not observed during conventional electric pacing (Fig. S8). One of the possible causes of pacing loss is overheating, because the heart may not cool effectively in an open chest. However, spontaneous pacing restoration during heating does not support this hypothesis. Long pacing of isolated cardiomyocytes demonstrated a similar effect: the pacing was spontaneously lost and restored during a long series, but finally, cells stopped responding (Fig. 5A). Since TRPV1 has significant conductivity for Ca^{2+} ions, we hypothesized that the possible cause of response termination was calcium overload. Immunostaining of tagged hTRPV1 demonstrated a significant fraction is localized in the endoplasmic reticulum (ER). ER and tagged hTRPV1 double staining with colocalization analysis gave us tresholded Mandel's coefficients tM1 = 0.292 and tM2 = 0.754, which means that almost 30% of all hTRPV1 is localized in ER, and 75% of the entire ER contains hTRPV1 (Fig. 5B–E). We used the genetically encoded calcium sensor GCaMP6s to visualize calcium dynamics inside cardiomyocytes both in calcium-containing and calcium-free media. In both cases, after the initial synchronization of calcium spikes with heat pulses, cells then lost synchronization, and demonstrated a rise in intracellular calcium together with loss of calcium spiking activity (Fig. 5F). This data demonstrates that ER-localized hTRPV1 may allow calcium to move from the ER to the cytosol causing calcium overload during pacing.

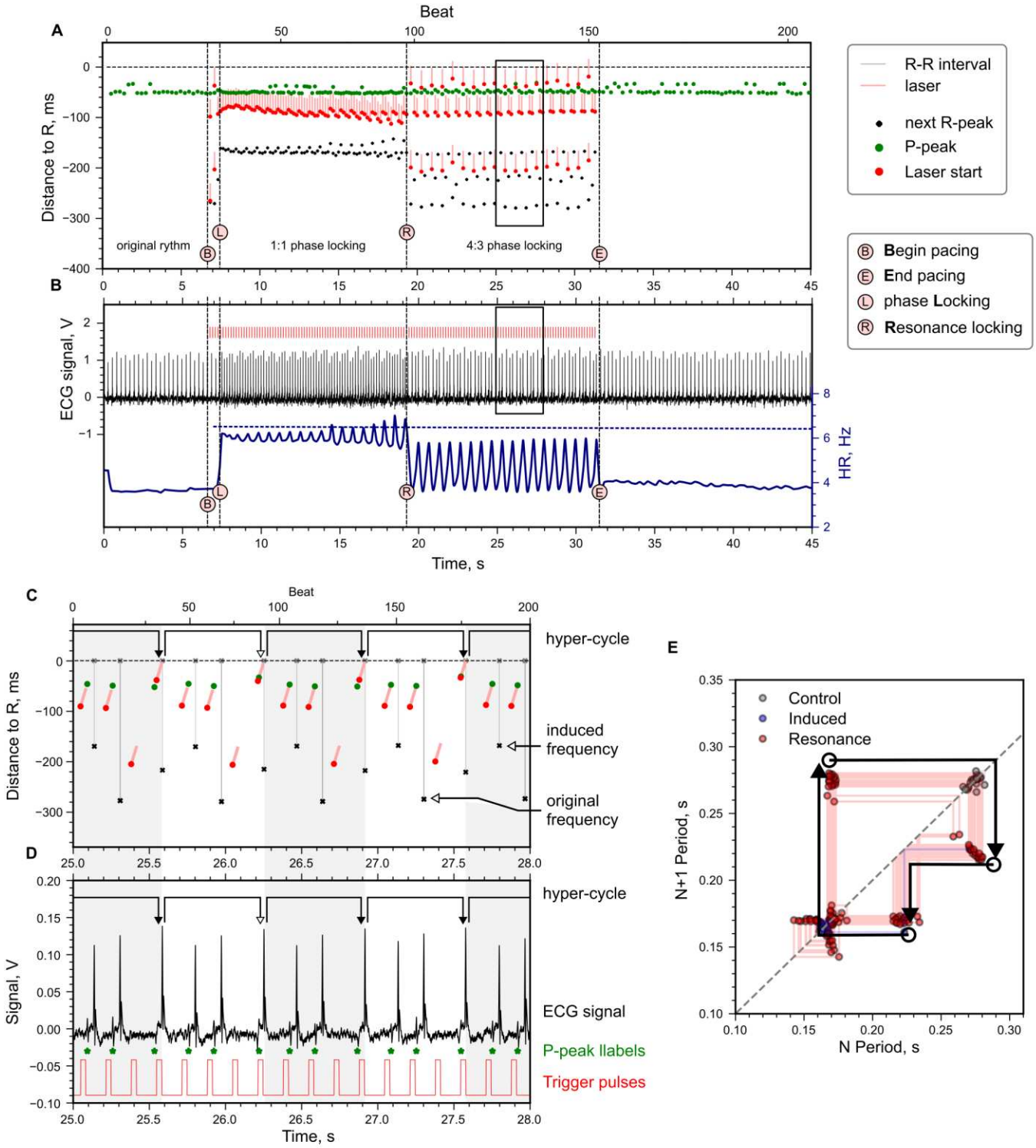

Figure 4. Characteristic example of pacing atrium with frequency where normal pacing is turned to the resonance. Pacing was at 6 Hz with 33 ms pulses, intrinsic HR was about 4 Hz. **A.** Position in ms of the P-peak, laser pulse and previous R-peak in relation to the next R-peak. The black frame shows the window zoomed at pane *C*. Critical events are marked with circled letters (see the legend). **B.** Change of complex shape (black curve) and heart rate (blue curve) during the experiment. Vertical red lines demonstrate trigger pulses. **C-D.** Same as **A–B** shown in a larger zoom in a region of 4:3 resonance. Hypercycles consisting of 3 R–R intervals are shown with arrows and a white/light gray background. **E.** Poincare diagram: next R-R interval plotted against previous one. Consequent points are connected by thin lines. The average 3-point hypercycle is shown with bold arrows.

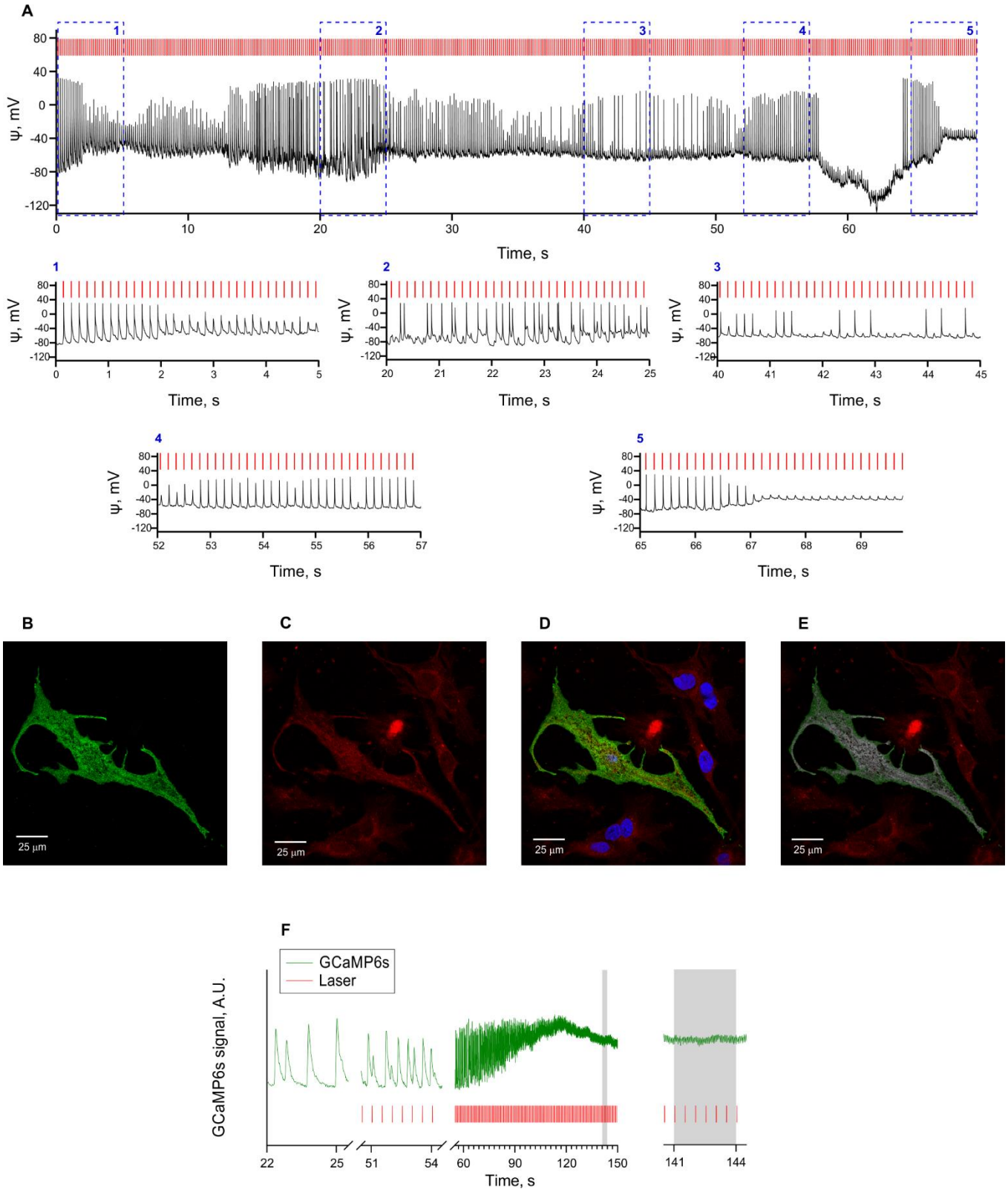

Figure 5. Long pacing, hTRPV1(−109aa) localisation and calcium dynamics upon heating in murine neonatal cardiomyocytes. A. Action potentials of an isolated neonatal murine cardiomyocyte during long pacing. **B–E.** Cellular localization of hTRPV1 in transduced neonatal murine cardiomyocytes. **B.** Staining of TRPV1-FLAG with anti-FLAG antibodies. **C.** Staining of ER with ER-tracker Red. **D.** Merged image. **E.** Colocalization of anti-FLAG and ER-tracker staining (shown in grays). **F.** Calcium pulses in a neonatal murine cardiomyocyte transduced with TRPV1(−109 a.a.) and heated by IR laser with a repetition rate of 2 Hz and 30 ms pulse width in calcium-free medium.

Discussion

In the present study, we demonstrated for the first time that thermogenetics can be applied for cardiac pacing. This technology opens the way for the search of new heart rhythm control and defibrillation strategies.

Thermogenetics is quite similar to optogenetics, but utilizes ion channels activated by temperature instead of light. In previous studies, optogenetics was successfully used to control the heart muscle *in vitro* and *in vivo*. In 2010, Bruegmann et al. were the first to demonstrate the possibility of heart rhythm control in mammals using transgenic mice expressing channelrhodopsin-2[10]. Five years later, this group, as well as Nussinovitch and Gepstein, demonstrated the possibility of using AAVs for the channelrhodopsin-2 gene delivery to the heart[11,12]. Over the next ten years, cardiac optogenetic developed extensively, which led to the creation of "all-optic cardiac electrophysiology"[30]. Nevertheless, the major problems of optogenetics — the low penetrance of the visible light and the immunogenity of opsins — remained unsolved.

Thermogenetics uses temperature sensitive channels which are expressed in non-immune-privileged tissues. We have shown that human TRPV1 can be used as a molecular tool for this technology, which opens possibilities for potential therapeutic methods in various fields of medicine in the future. TRPV1 activation was confirmed using the patch clamp method, as well as the genetically encoded fluorescent indicator GCAMP6S, which visualizes an increase in calcium flux. This channel is well-characterized and was successfully used in several studies for brain stimulation with magnetic fields heating nanoparticles in tissue[27,31,32]. TRP channels can be activated in various ways: by using chemical agonists such as capsaicin, by changing the ambient temperature[33–35] causing a change in the temperature of the whole animal, or by using IR laser stimulation[22,24,36]. In our study, the use of an IR laser setup made it possible to achieve a high spatial resolution, a fast channel activation rate, and wide possibilities for regulating the radiation intensity and duration of stimulation, which, if necessary, makes it possible to adapt this system to a wide variety of cells, tissues, and organisms. Moreover, recent studies demonstrate the possibility of heating freely moving mice's brains by focused ultrasound[37,38]. This technique may make truly non-invasive heart pacing possible, but it must be considered that in addition to heating, this technology includes cavitation and mechanical effects[39].

Excessive intake of calcium into the cell cytosol from the ER during stimulation of cardiomyocytes with the IR laser is the important factor limiting the duration of thermogenetic pacing. As a result, pacing is short-term, however we suggest that despite this, the technology has great potential for translational studies. A possible way to overcome this limitation is to use engineered TRPV1 channels with lower calcium conductance and lower ER tropism. Such channels will cause cell depolarization primarily due to the sodium inward current, preventing calcium overload. Another way could be to use multipoint laser heating with several pacing initiation sites in different areas of the heart. In this case, the points would be heated sequentially over a short time interval. This approach will avoid calcium overload of each individual point due to the additional rest time obtained and the normalization of calcium concentration in the cytosol. Another possible way to overcome current limitations is to target TRPV1 to specific cell types, such as pacemaker cells[40], Purkinje fibers[41], or cardiac ganglia[42]. The use of one of the proposed approaches or their use in combination may contribute to longer and more effective pacing.

The current setup cannot guarantee stable and complete 1:1 phase locking during pacing probably because of the effects described above. It occurs when the stimulation strength at the available maximum appears to be still weak. Interestingly, this "weak" stimulation sometimes bears resonance phase locking of 4:3 / 3:2 which are described by us for the first time in literature. Weak electric stimulation also produces resonance locks[43,44] but their numbers are different because the mechanism of stimulation is different. This phenomenon itself is very interesting to study in the context of arrhythmia genesis.

The electrophysiology of the heart in mice differs from larger mammals, including humans. Thus, the mice's heart rate is higher, so in humans, heart tissue has more time for cooling down and Ca^{2+} efflux from the cytosol. Since methods for gene delivery into myocardium are developing rapidly, the thermogenetic platform we present is capable of scaling to larger animals. This allows further research which is needed to establish the clinical perspectives of the method.

In the present study we used thermogenetics for heart pacing. It was demonstrated before that optogenetics can be used for the termination of ventricular arrhythmias in the whole heart[45]. Similar use of thermogenetics can help to develop methods for non-invasive and painless cardioversion.

This is the first study on cardiac thermogenetics. We believe that our approach holds promise not only for basic research but also for translational medicine.

Methods

Genetic constructs and viruses

In the present work, we used adeno-associated viruses (AAVs) serotype PHP.S[46] and DJ serotype[47] for cTnT gCaMP6s construction. The construction pUCmini-iCAP-PHP.S for AAV-PHP.S serotype assembly was kindly gifted by Viviana Gradinaru (Addgene plasmid #103006). For targeted expression of constructs in cardiomyocytes, we used a specific promoter — a constitutive hybrid promoter composed of the CMV immediate-early enhancer fused to the cardiac troponin T (cTnT) promoter. The plasmid containing cTnT was kindly gifted by Thomas Michel; Addgene plasmid #119164. pAAV cTnT hTRPV1 (−109 amino acids residues) P2A mRuby2 (P2A — a self-cleaving peptide), pAAV cTnT hTRPV1 3×FLAG tag and pAAV cTnT GCaMP6s were constructed for this work. All genetic constructs were assembled by AQUA-cloning[48]. pAAV cTnT HyPerDAAO plasmid was cleaved with SacI (Thermo Scientific, FD1133) and BglII restriction enzymes (Thermo Scientific, FD0083) to remove HyPerDAAO. For further assembly, the linearised vector was used. Genes encoding GCaMP6s and mRuby2 were amplified from plasmids previously generated in our laboratory.

The creation of short hTRPV1 (−109 amino acid residues) was based on the available pCAG_hTRPV1-p2A-tdTomato construct. The DNA sequence between the XbaI (Thermo Scientific, FD0684) and XhoI (Thermo Scientific, FD0695) restriction sites, with fragments of the chimeric intron and channel sequence, was inserted into the pAL2-T vector (Evrogen, TA002). Using the Tersus Plus PCR kit (Evrogen, PK221), blunting of the protruding ends in combination with A-tail treatment was performed. The overall construct was used to generate several short channel variants, including pCAG_(−109aa)hTRPV1-p2A-tdTomato. Then, a PCR reaction was performed. The PCR product was extracted using the Cleanup Standard kit (Evrogen, BC022S), and then treated with T4 polynucleotide kinase (Thermo Scientific, EK0031) and ligated. As a result, the sequence containing the chimeric intron and truncated channel fragments was cloned from the initial pAL2-T vector into pCAG_hTRPV1-p2A-tdTomato using XbaI and SmaI (Thermo Scientific, FD0663) restriction sites.

Construct verification was performed by sequencing. Midiprep was prepared using the Plasmid Midiprep 2.0 kit (Evrogen, #BC124) according to the manufacturer's instructions.

The 5′-end of primers was homologous to the vector and the 3′-end was specific to the particular sequence. The home-made chemically competent *Escherichia coli* Top10[49] strain was used for the cloning, maintenance, and propagation of plasmids. Overall, the acute assembly of the constructs and absences of mutations were verified by sequencing (Evrogen). Midipreps were prepared using the Plasmid Midiprep 2.0 kit (Evrogen, #BC124) according to the manufacturer's instructions. Then, constructs were packaged into AAV viral particles at the Viral Core Facility of Shemyakin-Ovchinnikov Institute of Bioorganic Chemistry. Virus titers were $2.1 \cdot 10^{12}$ and $6.2 \cdot 10^{12}$ VG/ml for pAAV cTnT hTRPV1 (–109 amino acids residues) P2A mRuby2, $2.1 \cdot 10^{12}$, $1.6 \cdot 10^{12}$, $8.1 \cdot 10^{12}$, $6.1 \cdot 10^{12}$, $9.1 \cdot 10^{12}$ VG/ml for pAAV cTnT hTRPV1 3×FLAG tag, $3.6 \cdot 10^{12}$ for pAAV cTnT gCaMP6s.

Cell cultures and transduction

The mixed mouse primary neonatal cardiomyocyte cell culture was obtained using a neonatal heart dissociation kit (Miltenyi Biotec, 130-098-373) according to the manufacturer's instructions. The cells were cultured in Dulbecco's Modified Eagle's Medium/Nutrient Mixture F-12 Ham (DMEM/F12), 1:1 mixture (BioloT, 1.3.7.2.) supplemented with 10% fetal bovine serum (FBS, Biosera, FB-1001/500), penicillin 100 U/ml /streptomycin 100 mg/ml (PanEko, A065п), and L-glutamine 0.365 g/l (PanEko, Ф032). The culture was seeded on 10mm microscope glass coverslips (Heinz Herenz, 1051199), which were coated with 10 mg/ml gelatin from bovine

skin (Sigma-Aldrich, G9391-100G) diluted in phosphate-buffered saline (PBS, PanEko, P071-1/B-60201) and maintained at 37°C in 5% CO_2. For transient expression of the hTRPV1 channel, a reporter protein, and a fluorescent Ca^{2+} sensor GCaMP6s, we used AAV-based vectors with the encoded genes above. For infection of the cardiomyocytes, we used AAV-DJ serotype at a MOI of 12,000 VG/cells for cTnT_hTRPV1(sh)_P2A_mRuby based viruses, and a MOI of 2,500 VG/cells for cTnT_GCaMP6s ones. The cells were infected on the next day after plating, and the transgene expression peak was observed on the third day after the infection.

TRPV1 channel localization

To understand the localization of the expressed TRPV1 channels in neonatal mice cardiomyocytes, we utilized cells infected with AAV-PHP.S serotype viruses with pAAV_cTnT_hTRPV1_P2A_FLAG-tag at a MOI of 2500 VG/cells. To visualize endoplasmic reticulum, we stained the live cells with ER-Tracker™ Red (BODIPY™ TR Glibenclamide, Thermo Fisher Scientific, E34250) according to the manufacturer's instructions. After the staining with ER-tracker, cardiomyocytes were fixed with 4% paraformaldehyde (Sigma-Aldrich, 158127-100G) for 5 minutes at room temperature and washed trice with 0.3% Tween 20 (Sigma-Aldrich, P1379-250ML) diluted in PBS (5 minutes each). The fixed cells then were blocked with PBS containing 0.12% tween 20, 1% bovine serum albumin (BSA, PanEko, 68100.10r), and 10% goat serum (Thermo Fisher Scientific, 16210072) for 40 minutes at room temperature. After the buffer removal, the cardiomyocytes were labeled with of DYKDDDDK Tag Recombinant Rabbit Monoclonal Antibody (8H8L17, Invitrogen, MA1-142-A488) at 1:500 dilution in 1% BSA, 10% goat serum, and 89% PBS for 2 hours at room temperature. The samples were washed three times with PBS after the incubations. Then, the cells were stained with Goat anti-Rabbit IgG (H+L) Cross-Adsorbed Secondary Antibody Alexa Fluor™ 488 (Invitrogen, A-11008) at dilution 1:500 for 1 hour at room temperature. The removal of non-conjugated antibodies was performed in parallel with cell nuclei staining. The cells were incubated with PBS supplemented with 2 µg/ml DAPI (Miltenyi Biotec, 130-111-570) for 15 minutes at room temperature. For further experiments, glasses with the labeled cells were placed onto the Superfrost Plus adhesion slides (Epredia, EPBRSF41296SP) in 20 µl VECTASHIELD Vibrance Antifade Mounting Media (Vector Laboratories, H-1700-2) and stored at +4°C in the dark.

The samples were analyzed using an inverted Nikon A1 confocal microscope and visualized using Nikon NIS-Elements software. We pictured the sample in each channel individually exciting DAPI, DYKDDDDK Tag-Alexa Fluor 488, and ER-tracker by laser lines 405 nm, 488 nm and 561 nm, respectively. Colocolization analysis was performed using ImageJ software.

Electrophysiology of single cardiac cells

Patch electrodes were pulled from hard borosilicate capillary glass (Sutter Instruments flaming/brown micropipette puller) and filled with an intracellular solution consisting of (in mM) K-gluconate, 100; KCl, 40; HEPES, 10; NaCl, 8; MgATP, 4; MgGTP, 0.3; phosphocreatine, 10 (pH 7.3 with KOH) in some experiments EGTA (15mM) was added to the intracellular solution. Cells were identified visually using IR-video microscopy using a Hamamatsu ORCA-Flash4.0 V3 Digital sCMOS camera (Hamamatsu Photonics) expression of wild type or mutant TRPV1 in the cardiomyocytes was confirmed by the presence of RFP. Coverslips were placed in a recording chamber continuously perfused with heated Tyrode's solution. Whole-cell recordings were taken at 32°C in current-clamp mode using a HEKA EPC-10 amplifier (List Elektronik) with a sampling rate of 100 µs. Steady state current was injected to achieve a membrane potential of approximately -60 to −90 mV. For experiments with capsaicin, it was applied directly to the cell via micropipette. For experiments using the IR laser the optic fiber was placed near the cell, and light from a green laser diode was shone onto the cell to check correct positioning. The laser was controlled via the TTL output from the HEKA EPC-10 amplifier. Laser intensity was chosen to achieve the desired temperature.

Intracellular calcium recordings of single cardiac cells

Neonatal cardiomyocyte cells transduced with GCaMP6s sensor were viewed and acquired under a water immersion Olympus LUMPLFLN40×W objective with 40X magnification. Data acquisition was performed at 20

fps using a Scientifica SliceScopePro 2000 microscope (Scientifica, UK) equipped with a Hamamatsu Orca Flash 4.0 CMOS monochrome digital camera (Hamamatsu Photonics) connected to a PC running the free software uManager. A CoolLED pE-300ultra was used as a light source. It was synchronized with the laser heating system via BNC-TTL output from the Heka Elektronik EPC 10 USB Patch Clamp Amplifier. The GCamp6s signal was analyzed using Fiji and GraphPad Prism 8 software.

Mice

Experiments were carried out using C57Bl/6J mice (The Jackson Laboratory, #000664, RRID: IMSR_JAX:000664) in compliance with all the ethical regulations for work with experimental animals and according to the European Convention for the Protection of Vertebrate Animals used for Experimental and other Scientific Purposes (1986, ETS 123). The animals were bred and housed in the animal facilities of the Institute of Bioorganic Chemistry of the Russian Academy of Sciences (IBCh RAS) in a 12 h light-dark cycle with free access to food and water. All procedures were approved by IBCh IACUC protocols No. 356 and No. 358.

Electrocardiography of immobilized mice

The principal scheme is illustrated in Fig. S5. The setup consisted of a laser source (assembled as described in section “Distant heating systems”), a JDS6600 electrical stimulator (Simac Electronics, Germany), external 10-MHz ADC E20-10 (L-CARD, Moscow, Russia), an IT-24P ultra-fast type T thermocouple (Physitemp, NJ, USA), an external High-Pass filter (handmade), two DPA-2FS biopotential amplifiers (NPI Electronics, Germany), one LP-04-M fixed-gain preamplifier (L-CARD, Moscow, Russia), a PC with PowerGraph 3.x preinstalled (DiSoft, Moscow, Russia), a homeothermic monitoring system (ThermoStar, China), and a SAR-1000 small animal ventilator(CWE, USA).

The ECG was recorded in a 4-electrode scheme (‘R’, ‘L’, ‘RL’, and ‘LF’). The anesthetized mouse was immobilized onto a homeothermic monitoring system, and F9049 disposable sticky electrodes (FIAB, Italy) were mounted to fix each paw on the mat. Each paw was preliminarily treated with keratinase (VEET, France) for better electrical contact. For recording, we used two differential amplifiers: we fed the R and L leads to their non-inverting inputs, and the LF lead to the inverting inputs. The RF lead was connected to the ground of the amplifiers, as well as to the screen of the foil surrounding the mouse from the bottom and sides. High-pass and low-pass frequencies were set to 0.3 and 10 kHz respectively, 100x gain was used. The output signal was additionally processed with a 0.1 Hz High-pass filter. The E20–10 ADC was operated with a 25 kHz sampling frequency mode per channel and 12-bit resolution. PowerGraph was set to remove 50-Hz interference from the mains using a digital band-cut filter (48–52 Hz) from both ECG signals (R–LF and L–LF). After band cutting, PowerGraph was instructed to subtract one input from another to calculate the R–L ECG signal, which was visualized and further saved to CSV files for programmatic analysis (see “Raw ECG data analysis”).

To synchronize laser pulses with the ECG signal, we operated the laser diode driver (LaserSource 4320) through its modulation input with the electrostimulator and fed the same trigger pulses to the separate channel of the ADC (Fig. S6, IN_4). To prevent the stimulator from interfering with the recorded signal, it was not connected to the main grid and received power from a powerbank staying galvanically isolated. The LD driver provides a time delay of less than 1 μs between the trigger pulse and operational current pulse, which is much lower than the time scale of the observed effects.

To control the temperature with high time resolution, we used an ultrasmall IT-24P T-couple (time constant 4 ms). This sensor was connected to a differential preamplifier (Fig. S6, LP-04-M). We did not use cold junction compensation for external temperature correction; therefore, we calibrated our thermocouple before every measurement, using a solid-state thermostat. To avoid possible negative effects caused by the thermocouple implantation, we only recorded temperature in control mice. We used the same IR laser modes for experimental and control animals.

Viral vector delivery

The viral vectors were delivered to mice hearts by an injection into the jugular vein. 6–8-week-old female mice were anesthetized with 5% isoflurane (Baxter, 10019036040) in an induction chamber (SomnoSuite, Kent Scientific), and then placed in the supine position onto a heating pad (Digital stereotaxic instrument, Stoelting Co). For deep anesthesia 1.5% isoflurane was administered through an inhalation mask during the operation. The hair was removed from the thorax with a trimmer, and the operating field was treated with 70% ethanol. Prior to incision, 0.25% of local anesthetic bupivacaine (Ozon) was injected into the area lateral to the midline of the body. After several minutes, a small incision was made from the pectoral muscle to the lower part of the neck. Adeno-associated viruses were injected into the jugular vein using insulin syringes with a 27-gauge needle. Each animal was injected with approximately 100 µl of a suspension of pAAV_cTnT_hTRPV1_FLAG-tag AAV-PHP.S serotype viral particles for a total of $4–6 \cdot 10^{11}$ genomes per mouse. The wound was sutured, and the mice were intraperitoneally injected with ketoprofen (5 mg/kg, Sandoz). For recovery, animals were placed in individual cages for at least a month.

Detection of the TRPV1 expression in mice heart

Expression of TRPV1 channel in cardiac tissue after intravenous injections of pAAV_cTnT_hTRPV1_P2A_FLAG-tag in mice was confirmed by immunohistochemical staining of slices. The mice were deeply anesthetized with 3% isoflurane and decapitated, the hearts were isolated and placed in Tissue-Tek Cryomold (Sakura Finetek, 62534-10) filled with Tissue-Tek O.C.T. Compound (Sakura Finetek, 4583). The mold with the heart was frozen in liquid nitrogen vapor and then stored at −80°C or immediately dissected into thin 15 µm sections using an HM525 NX cryostat (Thermo Scientific) at −15°C. The prepared samples were placed onto the Superfrost Plus adhesion slides and stored at −20°C.

Heart tissues were fixed in 4% paraformaldehyde in PBS for 5 minutes at room temperature and then washed with 0.3% Tween 20 in PBS three times with further incubation for 5 minutes. To block nonspecific binding, slices were incubated in a blocking buffer (10% goat serum, 1% bovine serum albumin, 0.15% Tween 20, PBS) for 1 hour at room temperature, then washed again with 0.3% Tween 20, PBS. Staining with DYKDDDDK Tag Recombinant Rabbit Monoclonal Antibody (8H8L17, Invitrogen, 701629) at 1:500 dilution was performed in blocking solution at 4°C for 14 hours. Slices were then washed three times with 0.3% Tween 20, PBS. Incubation with Goat anti-Rabbit IgG (H+L) Cross-Adsorbed Secondary Antibody Alexa Fluor™ 647 (Invitrogen, A-21244) in 1:500 dilution was also performed in a blocking buffer for 2 hours at room temperature. The stained samples were incubated for 15 minutes in PBS supplemented with 2 µg/ml DAPI and washed by distillate water once. The slides with the stained slices were covered with 10mm microscope glass coverslips with 20 µl VECTASHIELD Vibrance Antifade Mounting Media. The specimens were stored in the dark at +4°C.

The localization of hTRPV1 in immunocytochemically stained cardiomyocytes was analyzed by confocal microscopy via an inverted Nikon A1 confocal microscope and visualized using Nikon NIS-Elements software. For DAPI excitation, a 405 nm laser was used, and for Alexa647 excitation — 633 nm.

Raw ECG data analysis

CSV files containing one or two ECG channels and laser trigger pulse channel were generated using PowerGraph with a 10kHz sampling rate. Initial R-peak annotation was performed using *neurokit2*[50], then the annotation was manually corrected with PhysioZoo interface[51]. Further processing was performed using hand-made python3 scripts with *neurokit2* and standard libraries for data analysis. *scipy.signal* and *scipy.ndimage* subpackages were used to operate 1D data. Heart rate smooth dependency over time plotted in Fig. 2,3 and others was calculated by applying 1-dimensional Gaussian filter with σ=2s to discrete heart rate data (inverted sizes of RR interval against start time of the R-peak). ECG denoising was performed with PCA (implemented in *scikit-learn* package). Each RR interval were resampled to an average RR length, then PCA was performed and 3 first PCs was used to reconstruct RR interval; next, an interval was resampled back to its original length. During the analysis of pacing data, PCA was performed separately for RR intervals under laser treatment and for control RR intervals. PCA-

denoised data were then delineated with *neurokit2* using continuous wavelet transform method to annotate P-peaks.

Distant heating systems

Two optical systems were used to stimulate cardiomyocytes *in vitro* and *in vivo*. Both were equipped with a fiber coupled laser diode (LD) 4PN-117 (SemiNex) as a powerful heating laser, providing radiation at a wavelength of 1375 nm with an average power of up to 4.3 W through a multimode fiber with a core diameter of 105 μm and 0.22NA. The LD was mounted onto a TEC-controlled plate "264 TEC HP LaserMount" (Arroyo Instruments, A.I.), which was operated by TEC driver TECSource 5305 (A.I.); current stabilization and control for LD were performed with LD driver LaserSource 4320 (A.I.). For pulse-mode heating, an external pulse trigger was used (see "Electrocardiography of immobilized mice" section).

For cell culture heating an all-fiber system was developed. To illuminate the heating region, we used a PL520 (Thorlabs) laser diode at a wavelength of 520 nm, which was optically conjugated with the tip of a 200-μm 0.22NA FG200UEA (Thorlabs) optical fiber by optical glue. Combining IR and visible radiation was performed using 90:10 splitters TM105R2F2B (Thorlabs) for fibers with a diameter of 105 μm 0.22NA and reduced OH content. For optimal transmission of IR radiation, it was fed into the Signal channel with a 90% power transmission. The splitter's auxiliary output could be used to monitor the IR power. The main channel was connected to a 2-m-long optical fiber, which supplied IR radiation to the object, with parameters 105 μm/0.22NA (FG105LCA, Thorlabs). Due to low-OH content, the fiber had increased transmission in the IR range, which made it possible to reduce losses by ~100 times. All light guide elements had connectors, which made it possible to securely connect them to each other. The overall IR power transfer efficiency was 65%. This laser heating system was synchronized with the recording of cell membrane potentials and currents through them using a low-noise amplifier HEKA EPC 10 USB. The end of the fiber was placed on a three-coordinate manipulator (Stoelting). The expansion cone of IR radiation in the solution was ~9°, which led to an elliptical heating spot 150×300 μm at a distance of 200 μm from the cells. In experiments on pulsed heating, the IR power reached 2.1 W and the intensity up to 6 kW/cm^2 (at a maximum control voltage of 2.5 V).

When a heart was stimulated, LD IR laser radiation was free space coupled using an F810SMA-1310 collimator (Thorlabs). This allowed the IR radiation to be combined with emission of a green laser diode at a wavelength of 532 nm CPS532-C2 (Thorlabs) with a power about 1 mW on a DMLP1000 dichroic mirror (Thorlabs) to visualize the heated area. The infrared and visible light was coupled to a 2-m-long FT800EMT (Thorlabs) glass fiber with the core diameter 800 μm and the numerical aperture 0.39NA with a reduced OH content to reduce absorption in the 1350–1500 nm region by a lens with a focal length of 50 mm. To heat the tissue, the end tip of the IR grade light guide was set at a distance of 6 to 8 mm from the surface of the heart, which created a heating spot with a diameter of 1.9 mm to 2.6 mm. The overall efficiency of energy delivery to the heart was ~70%. In the continuous heating mode, the power varied from 250 mW (controlling voltage is 0.6 V) to 600 mW (1.0 V), which led to heating from 32 °C to 37–43 °C. When heated by pulses, the peak power rose to 1.3 W.

References

1. Timmis, A. et al. European Society of Cardiology: Cardiovascular Disease Statistics 2019. Eur. Heart J. 41, 12–85 (2020).

2. Glikson, M. et al. 2021 ESC Guidelines on cardiac pacing and cardiac resynchronization therapy. Eur. Heart J. 42, 3427–3520 (2021).

3. Ranasinghe, I. et al. Institutional Variation in Quality of Cardiovascular Implantable Electronic Device Implantation: A Cohort Study. Ann. Intern. Med. 171, 309–317 (2019).

4. Marbán, E. & Cho, H. C. Biological pacemakers as a therapy for cardiac arrhythmias. Curr. Opin. Cardiol.

23, 46–54 (2008).

5. Cho, H. C. & Marbán, E. Biological therapies for cardiac arrhythmias: Can genes and cells replace drugs and devices? Circ. Res. 106, 674–685 (2010).

6. Rosen, M. R., Robinson, R. B., Brink, P. R. & Cohen, I. S. The road to biological pacing. Nat. Rev. Cardiol. 8, 656–666 (2011).

7. Jia, Z. et al. Stimulating cardiac muscle by light cardiac optogenetics by cell delivery. Circ. Arrhythm. Electrophysiol. 4, 753–760 (2011).

8. Nussinovitch, U., Shinnawi, R. & Gepstein, L. Modulation of cardiac tissue electrophysiological properties with light-sensitive proteins. Cardiovasc. Res. 102, 176–187 (2014).

9. Arrenberg, A. B., Stainier, D. Y. R., Baier, H. & Huisken, J. Optogenetic control of cardiac function. Science 330, 971–974 (2010).

10. Bruegmann, T. et al. Optogenetic control of heart muscle in vitro and in vivo. Nat. Methods 7, 897–900 (2010).

11. Nussinovitch, U. & Gepstein, L. Optogenetics for in vivo cardiac pacing and resynchronization therapies. Nat. Biotechnol. 33, 750–754 (2015).

12. Vogt, C. C. et al. Systemic gene transfer enables optogenetic pacing of mouse hearts. Cardiovasc. Res. 106, 338–343 (2015).

13. Lin, J. Y., Knutsen, P. M., Muller, A., Kleinfeld, D. & Tsien, R. Y. ReaChR: A red-shifted variant of channelrhodopsin enables deep transcranial optogenetic excitation. Nat. Neurosci. 16, 1499–1508 (2013).

14. Klapoetke, N. C. et al. Independent optical excitation of distinct neural populations. Nat. Methods 11, 338–346 (2014).

15. Prakash, R. et al. Two-photon optogenetic toolbox for fast inhibition, excitation and bistable modulation. Nat. Methods 9, 1171–1179 (2012).

16. Dawydow, A. et al. Channelrhodopsin-2-XXL, a powerful optogenetic tool for low-light applications. Proc. Natl. Acad. Sci. U. S. A. 111, 13972–13977 (2014).

17. Feldbauer, K. et al. Channelrhodopsin-2 is a leaky proton pump. Proc. Natl. Acad. Sci. U. S. A. 106, 12317–12322 (2009).

18. Maimon, B. E. et al. Optogenetic Peripheral Nerve Immunogenicity. Sci. Rep. 8, 14076 (2018).

19. Richter, C. & Bruegmann, T. No light without the dark: Perspectives and hindrances for translation of cardiac optogenetics. Prog. Biophys. Mol. Biol. 154, 39–50 (2020).

20. Bernstein, J. G., Garrity, P. A. & Boyden, E. S. Optogenetics and thermogenetics: Technologies for controlling the activity of targeted cells within intact neural circuits. Curr. Opin. Neurobiol. 22, 61–71 (2012).

21. Tominaga, M. & Calerina, M. J. Thermosensation and pain. J. Neurobiol. 61, 3–12 (2004).

22. Bath, D. E. et al. FlyMAD: Rapid thermogenetic control of neuronal activity in freely walking Drosophila. Nat. Methods 11, 756–762 (2014).

23. Roshchin, M. et al. Thermogenetic stimulation of single neocortical pyramidal neurons transfected with TRPV1-L channels. Neurosci. Lett. 687, 153–157 (2018).

24. Ermakova, Y. G. et al. Thermogenetic neurostimulation with single-cell resolution. Nat. Commun. 8, 1–15 (2017).

25. Safronov, N. A. et al. Microwave-induced thermogenetic activation of single cells. Appl. Phys. Lett. 106, 163702 (2015).

26. Kubanek, J. et al. Ultrasound modulates ion channel currents. Sci. Rep. 6, 1–14 (2016).

27. Chen, R., Romero, G., Christiansen, M. G., Mohr, A. & Anikeeva, P. Wireless magnetothermal deep brain stimulation. Science 347, 1477–1480 (2015).

28. Jappy, D. et al. Pacing of primary murine cardiomyocytes expressing human TRPV1 using infra-red laser. (2023) doi:10.5281/zenodo.10402004.

29. Balatskiy, A. et al. ECG recordings of cardiac pacing in mice carrying TRPV1. (2023) doi:10.5281/zenodo.8346874.

30. Entcheva, E. & Kay, M. W. Cardiac optogenetics: a decade of enlightenment. Nat. Rev. Cardiol. 18, 349–367 (2021).

31. Hescham, S.-A. et al. Magnetothermal nanoparticle technology alleviates parkinsonian-like symptoms in mice. Nat. Commun. 12, 5569 (2021).

32. Munshi, R. et al. Magnetothermal genetic deep brain stimulation of motor behaviors in awake, freely moving mice. eLife 6, e27069 (2017).

33. Pulver, S. R., Pashkovski, S. L., Hornstein, N. J., Garrity, P. A. & Griffith, L. C. Temporal dynamics of neuronal activation by channelrhodopsin-2 and TRPA1 determine behavioral output in Drosophila larvae. J. Neurophysiol. 101, 3075–3088 (2009).

34. Vasmer, D., Pooryasin, A., Riemensperger, T. & Fiala, A. Induction of aversive learning through thermogenetic activation of Kenyon cell ensembles in Drosophila. Front. Behav. Neurosci. 8, (2014).

35. Chen, S., Chiu, C. N., McArthur, K. L., Fetcho, J. R. & Prober, D. A. TRP channel mediated neuronal activation and ablation in freely behaving zebrafish. Nat. Methods 13, 147–150 (2016).

36. Keene, A. C. & Masek, P. Optogenetic induction of aversive taste memory. Neuroscience 222, 173–180 (2012).

37. Yang, Y. et al. Sonothermogenetics for noninvasive and cell-type specific deep brain neuromodulation. Brain Stimulat. 14, 790–800 (2021).

38. Wang, L. et al. The Noninvasive Sonothermogenetics Used for Neuromodulation in M1 Region of Mice Brain by Overexpression of TRPV1. Neuroscience 527, 22–36 (2023).

39. King, R. L., Brown, J. R., Newsome, W. T. & Pauly, K. B. Effective parameters for ultrasound-induced in vivo neurostimulation. Ultrasound Med. Biol. 39, 312–331 (2013).

40. Lee, F. K. et al. Genetically engineered mice for combinatorial cardiovascular optobiology. eLife 10, (2021).

41. Zaglia, T. et al. Optogenetic determination of the myocardial requirements for extrasystoles by cell type-specific targeting of ChannelRhodopsin-2. Proc. Natl. Acad. Sci. U. S. A. 112, E4495–E4504 (2015).

42. Rajendran, P. S. et al. Identification of peripheral neural circuits that regulate heart rate using optogenetic and viral vector strategies. Nat. Commun. 10, 1–13 (2019).

43. Guevara, M. R., Glass, L. & Shrier, A. Phase Locking, Period-Doubling Bifurcations, and Irregular Dynamics in Periodically Stimulated Cardiac Cells. Science 214, 1350–1353 (1981).

44. Chialvo, D. R., Gilmour Jr, R. F. & Jalife, J. Low dimensional chaos in cardiac tissue. Nature 343, 653–657 (1990).

45. Nyns, E. C. A. et al. Optogenetic termination of ventricular arrhythmias in the whole heart: towards biological cardiac rhythm management. Eur. Heart J. 38, 2132–2136 (2017).

46. Chan, K. Y. et al. Engineered AAVs for efficient noninvasive gene delivery to the central and peripheral nervous systems. Nat. Neurosci. 20, 1172–1179 (2017).

47. Grimm, D. et al. In Vitro and In Vivo Gene Therapy Vector Evolution via Multispecies Interbreeding and Retargeting of Adeno-Associated Viruses. J. Virol. 82, 5887–5911 (2008).

48. Beyer, H. M. et al. AQUA cloning: A versatile and simple enzyme-free cloning approach. PLoS ONE 10, e0137652 (2015).

49. Liu, J. et al. An Improved Method of Preparing High Efficiency Transformation Escherichia coli with Both Plasmids and Larger DNA Fragments. Indian J. Microbiol. 58, 448–456 (2018).

50. Makowski, D. et al. NeuroKit2: A Python toolbox for neurophysiological signal processing. Behav. Res. Methods 53, 1689–1696 (2021).

51. Behar, J. A. et al. PhysioZoo: A novel open access platform for heart rate variability analysis of mammalian electrocardiographic data. Front. Physiol. 9, 391349 (2018).

Acknowledgements

This research was funded by the Russian Science Foundation (RSF), grant number 23-75-10111. We thank the Group of redox biology IBCh RAS, particularly Viktoriya G. Krut', Liana F. Mukhametshina and Dmitry I. Maltsev for assistance in preparing hTRPV1 (−109 amino acid residues) data.

Author information

Authors and Affiliations

Shemyakin-Ovchinnikov Institute of Bioorganic Chemistry, Russian Academy of Sciences, Moscow, Russia
Aleksandr A. Lanin, Vera S. Ovechkina, Semyon S. Sabinin, Elena S. Fetisova, Rostislav A. Sokolov, Georgy M. Solius, Ekaterina M. Solius, Oleg V. Podgorny, Ilya V. Kelmanson, Andrey A. Mozhaev and Vsevolod V. Belousov

Federal Center of Brain Research and Neurotechnologies, Federal Medical Biological Agency, Moscow, Russia
Alexander V. Balatskiy, Alexey M. Nesterenko, Alexander A. Moshchenko, David Jappy, Rostislav A. Sokolov, Diana Z. Biglova, Sergey V. Korolev, Oleg V. Podgorny, Andrei V. Rozov and Vsevolod V. Belousov

Center for Precision Genome Editing and Genetic Technologies for Biomedicine, Pirogov Russian National Research Medical University, Moscow, Russia
Vera S. Ovechkina, Rostislav A. Sokolov, Oleg V. Podgorny, Ilya V. Kelmanson, Andrey A. Mozhaev and Vsevolod V. Belousov

M.V. Lomonosov Moscow State University, Moscow, Russia
Aleksandr A. Lanin, Andrei B. Fedotov

Federal Clinical Research Centre, Federal Medical Biological Agency, Moscow, Russia
Sergey V. Korolev

Institute for Cardiovascular Physiology, University Medical Center Göttingen, Göttingen, Germany
Tobias Bruegmann

German Center for Cardiovascular Research (DZHK), Partner site Göttingen, Göttingen, Germany
Tobias Bruegmann

Cluster of Excellence "Multiscale Bioimaging: from Molecular Machines to Networks of Excitable Cells" (MBExC), University of Göttingen, Göttingen, Germany
Tobias Bruegmann

Texas A&M University, College Station, Texas, United States
Aleksei M. Zheltikov

Federal Scientific Research Centre "Crystallography and Photonics", Russian Academy of Sciences, Moscow, Russia
Andrey A. Mozhaev

National Research University Higher School of Economics, Moscow, Russia
Andrey A. Mozhaev

Contributions

Conceptualization: S.V.K. T.B., and V.V.B; Data curation: A.V.B., A.M.N., D.J., R.A.S., and D.Z.B.; Formal analysis: A.M.N. and D.Z.B.; Funding acquisition: A.A.Mozh. and V.V.B; Investigation: A.V.B., A.M.N., A.A.L., V.S.O., S.S.S., E.S.F., D.J., R.A.S., I.V.K., A.V.R., and A.A.Mozh.; Methodology: A.V.B., A.M.N., A.A.L., E.S.F., R.A.S., I.V.K., A.V.R., A.B.F., A.M.Z., and A.A.Mozh.; Project administration: A.V.B., I.V.K., and V.V.B; Resources: A.A.L., A.A.Moshch., G.M.S., E.M.S., O.V.P., A.V.R., A.B.F., and A.M.Z.; Software: A.M.N. and D.Z.B.; Supervision: T.B. and V.V.B; Validation: A.V.B. and A.M.N.; Visualization: A.V.B., A.M.N., and D.J.; Writing – original draft: A.V.B., A.M.N., V.S.O., S.S.S., and A.A.Mozh.; Writing - review & editing: A.A.L., S.S.S., E.S.F., A.A.Moshch., D.J., R.A.S., S.V.K., O.V.P., I.V.K., A.V.R., T.B., and V.V.B.

Corresponding authors

Correspondence to Vsevolod V. Belousov

belousov@fccps.ru